Artificial Neural Network Models for Prediction of Density and Kinematic Viscosity of Different Systems of Biofuels and Their Blends with Diesel Fuel. Comparative Analysis

S. Belmadani,[a*] *S. Hanini,*[b] *M. Laidi,*[b] *C. Si-Moussa,*[b] and *M. Hamadache*[b]

[a] Department of Chemical Industry, University of Saad Dahlab of Blida 1, Algeria
[b] Laboratory of Biomaterials and Transport Phenomena (LBMPT), University of Médéa, Algeria

Abstract
In the present article, two models based on the artificial neural network methodology (ANN) have been optimised to predict the density (ρ) and kinematic viscosity (μ) of different systems of biofuels and their blends with diesel fuel. An experimental database of 1025 points, including 34 systems (15 pure systems, 14 binary systems, and 5 ternary systems) was used for the development of these models. These models use six inputs, which are temperature (T) in the range of $-10-200$ °C, volume fractions (X_1, X_2, X_3) in the range of 0–1, and to distinguish these systems, we used kinematic viscosity at 20 °C in the range of $0.67-74.19$ mm^2 s^{-1} and density at 20 °C in the range of $0.7560-0.9188$ g cm^{-3}. The best results were obtained with the architecture of {6-26-2: 6 neurons in the input layer – 26 neurons in the hidden layer – 2 neurons in the output layer}. Results of comparison between experimental and simulated values in terms of the correlation coefficients were: $R^2 = 0.9965$ for density, and $R^2 = 0.9938$ for kinematic viscosity. A 238 new database experimental of 4 systems (2 pure systems, 1 binary system, and 1 ternary system) was used to check the accuracy of the two ANN models previously developed. Results of prediction performances in terms of the correlation coefficients were: $R^2 = 0.9980$ for density, and $R^2 = 0.9653$ for kinematic viscosity. Comparison of validation results with those of the other studies shows that the neural network models gave far better results.

Keywords
Modelling, neural network, kinematic viscosity, density, biofuels

1 Introduction

According to the statistics, the total greenhouse gas (GHG) emissions associated with aviation will be 400 to 600 % higher in 2050 than in 2010.[1] In addition, it is imperative to reduce carbon dioxide (CO_2) emissions given their harmful impact on the environment. Over the last 10 to 20 years, these environmental concerns have led to the intensification of studies inherent to the search for alternatives to conventional fuels.[2]

Among the developed alternatives that have significantly lower greenhouse gas emissions than conventional fuel, biofuels are presented as an attractive renewable energy source that is environmentally friendly.[3] The raw materials used for the production of biofuels are of biological origin and are therefore renewable. Non-edible oilseed crops are the main resources available.[3]

Specifications and limits on physical properties of fuels are established in America by the American Society for Testing and Materials (ASTM specifications) and in Europe by the European Committee for Standardization (EN European Norm).[4]

Density and viscosity of biofuel are two important physical properties that define the quality of fuels.[5] The density of a substance is defined as its mass *per* unit volume. It is a physical property that is used for the design of storage tanks and pipes, and that calculates the precise volume of fuel needed to provide the adequate combustion. Viscosity is the physical property of a substance characterizing its resistance to flow. Viscosity influences the lubrication properties as well as the combustion properties of the fuel.

Low viscosities lead to poor lubrication, which can cause excessive wear and leakage. Higher viscosities can cause an obstruction of the hoses or poor atomization of the fluid leading to poor combustion and an increase in exhaust gas emissions.[4]

Physical and chemical properties of some compounds cannot be obtained directly or immediately from experiments due to experimental safety and efficiency.[6] The development of prediction methods are of great value in estimating properties of biofuel. Therefore, much research has been directed towards the design of models for the prediction of physical properties of different types and different systems of biofuel. For example, *Baroutian et al.*[7] proposed the empirical correlations to estimate viscosity and density of binary and ternary blends of palm oil + palm biodiesel + diesel fuel at different temperatures. *Chavarria-Hernandez et al.*[8] designed three complementary correlations to accurately predict the kinematic viscosity of FAMEs and biodiesel for a wide temperature range (263.15–373.15 K), and for a wide range of hydrocarbon chain length (C6 : 0–C24 : 0, including unsaturated FAMEs).

Few predictive studies of biofuel properties using artificial neural network models have been reported in the litera-

* Corresponding author: Souad Belmadani
Email: belmadanisouad2014@gmail.com

ture. For example, *Rocabruno-Valdés et al.*[9] predicted the density, dynamic viscosity, and cetane number of biodiesel using artificial neural networks. The authors used an array of 16 : 1 : 1 for the density of biodiesel, sixteen entries for the temperature, and the composition of each fatty acid methyl ester, C8 : 0 to C24 : 0 in biodiesel, 16 : 1 : 1 for the dynamic viscosity of biodiesel, 16 : 2 : 2 for the density–viscosity of biodiesel, 16 : 6 : 1 for the cetane number of biodiesel. More recently, various neural networks, including single layer neural network (SLNN), deep neural network (DNN) with multi-layers, and convolution neural network (CNN) have been developed by *Houet et al.*[6] to predict multiple molecular properties simultaneously.

For the prediction of all 15 molecular properties at a time, DNN with 3-layers network exhibits the best results. They concluded that the number of layers in DNN play a key role in the prediction of multiple molecular properties simultaneously.

Given the importance of viscosity and density prediction models, the main objective of this work was to develop a mathematical model using artificial neural network to estimate the density and kinematic viscosity of different types and different systems of biofuels and their blends with diesel fuel. The details of the calculation method, numerical validation, statistical analysis, and comparative analysis are fully described in this work.

2 Experimental

2.1 Density and viscosity

The general empirical correlations in the literature for the density and viscosity in function of temperature and volume fraction can be given by:

$$y = \exp(a_0 + a_1 X_v + a_2 X_v/T + a_3/T + a_4/T^2 + a_5 X_v/T^2 + a_6 T + a_7 X_v T) + a_8 T^3 + a_9 T^2 + a_{10} T + b_0 X_v + a_{11}, \tag{1}$$

where y is a kinematic viscosity (μ) in mm^2 s^{-1} or a density (ρ) in g cm^{-3}, b_0, a_0, a_1, a_2, ...a_{11} are constants, T is a temperature in K, and X_v is a volume fraction.

The values of (b_0, a_0, a_1, a_2,... a_{11}) for different systems in the literature are summarized in the Table 1.

2.2 Artificial neural networks

Neural network is a widely distributed parallel processor consisting of simple processing units (nodes) that perform certain mathematical functions, usually non-linear. This type of arithmetic calculated by the system is similar to the human brain structure. The great advantage of these models is their ability to learn, circulate, or extract rules automatically from the complex data.[13] In ANN applications, three stages are considered: (a) training, (b) validation, and (c) testing.[14]

In such ANN, a neuron in a hidden or an output layer has two tasks:[15] to sum the weighted inputs from several connections plus a bias value, and then to apply the transfer function to the sum (Fig. 1):

$$z_j = f_H \left(\sum_{i=1}^{n} E_i w_{i,j} + b_j \right); j = 1, 2, ..., m. \tag{2}$$

The output S_k:

$$S_k = f_O \left(\sum_{i=1}^{n} V_{k,j} z_j + b_k \right); k = 1, 2, ..., l. \tag{3}$$

Table 1 – Values of (b_0, a_0, a_1, a_2 ... a_{11}) for different systems in the literature

| Constants | Kinematic viscosity | | | | | | | | | Density | | | |
| | Ref. [10] | Ref. [11] | Ref. [12] | | | | | | | Ref. [10] | Ref. [11] | Ref. [12] | |
	Eq. (2)	Eq. (3)	Eq. (4)	Eq. (5)	Eq. (6)	Eq. (7)	Eq. (8)	Eq. (9)		Eq. (10)	Eq. (11)	Eq. (12)	Eq. (13)
b_0	0	0	0	0	0	0	0	0		0	0	0	b_0
a_0	0	0	a_0	a_0	a_0	a_0	a_0	a_0		0	0	0	0
a_1	0	0	0	0	a_1	a_1	a_1	a_1		0	0	0	0
a_2	0	0	0	a_2	0	0	0	a_2		0	0	0	0
a_3	0	a_3	a_3	a_3	a_3	a_3	0	a_3		0	0	0	0
a_4	0	0	a_4	0	0	0	0	0		0	0	0	0
a_5	0	0	0	0	a_5	0	0	0		0	0	0	0
a_6	a_6	a_6	0	0	0	0	a_6	0		0	0	0	0
a_7	0	0	0	0	0	0	a_7	0		0	0	0	0
a_8	0	0	0	0	0	0	0	0		a_8	0	0	0
a_9	0	0	0	0	0	0	0	0		a_9	0	0	0
a_{10}	0	0	0	0	0	0	0	0		a_{10}	a_{10}	a_{10}	a_{10}
a_{11}	0	a_{11}	0	0	0	0	0	0		a_{11}	a_{11}	a_{11}	a_{11}

Combining Eqs. 2 and 3, the relation between the output (S_k) and the inputs E_i of the ANN is:

$$S_k = f_O\left(\sum_{i=1}^{n} v_{k,j} f_H\left(\sum_{i=1}^{n} E_i w_{i,j} + b_j\right) + b_k\right); k = 1, 2, \ldots, l. \quad (4)$$

The output is computed by means of a transfer function (activation function). The typical activation functions which fulfil these requirements are:[15]

hyperbolic tangent transfer function:

$$f(x) = \frac{2}{1 + e^{-2x}} - 1, \quad (5)$$

identity transfer function:

$$f(x) = x. \quad (6)$$
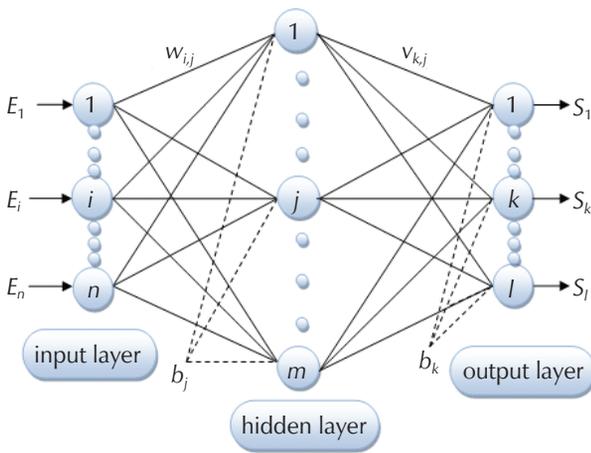
Fig. 1 – Schematic of a three-layer feedforward neural network, where E_i is the input of neuron i; $w_{i,j}$ is the synaptic weight of the connection from neuron i of the input layer to neuron j in the hidden layer; $v_{k,j}$ represents the weight of synaptic connection the neuron j of the hidden layer to neuron k of the output layer; b_j and b_k represent the means of neuron j in the hidden and the neuron k of the output layer; S_k is the output of neuron k.

2.3 Data acquisition and analysis

Databases of this study have been formed from the results reported in the literature. A total of 1025 data points were obtained from various scientific publications[10–12,16–24] to estimate the density and kinematic viscosity of different systems of biofuels and their blends with diesel fuel.

In this case, the database was divided randomly into three groups of 70 % for training, 15 % for testing, and 15 % for validating. Temperature, volume fraction, μ (at 20 °C), and ρ (at 20 °C) were considered as input variables of the artificial neural network.

The minimum (min) and maximum (max) values are presented in Table 2 and a general representation of an ANN with "six" number of inputs is shown in Fig. 2.

The list of pure, binary, and ternary systems, and the experimental data points for the density and kinematic viscosity of both systems that have been used in this study is presented in Table 3. In this work, the STATISTICA program was used for the application of the artificial neural network.

Table 2 – Limit values for the input and output variables on the ANN models

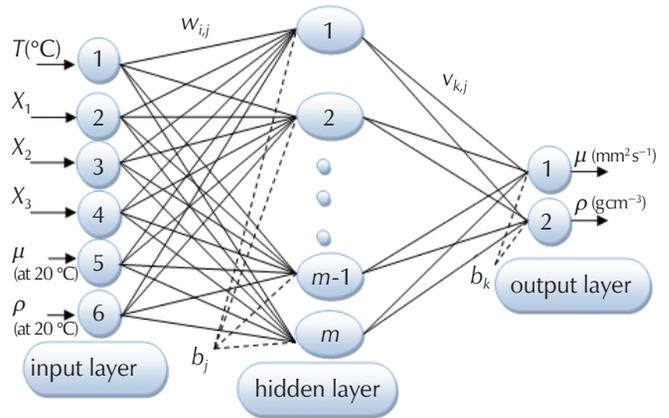|	Min	Max	Units
Input values			
temperature / T	−10	200	°C
volume fractions / X_1, X_2, X_3	0	1	volume fraction
density at 20 °C / ρ	0.7560	0.9188	$g\,cm^{-3}$
kinematic viscosity at 20 °C / μ	0.67	74.19	$mm^2\,s^{-1}$
output values			
density / ρ	0.7180	0.9259	$g\,cm^{-3}$
kinematic viscosity / μ	0.58	119.48	$mm^2\,s^{-1}$

Fig. 2 – ANN architecture used for estimation in the present work

2.4 Selection of optimal configuration

The performance of a trained network can be measured to some extent by the errors on the training, validation, and test data sets. Regression analysis has been applied to assess the network capability for density and kinematic viscosity predictions.

The coefficient of determination, R^2 (see Eq. (7)),[25,26] has been used as a measure to evaluate how the trained network estimation is correlated to the experimental data. Also, different neural network topologies have been compared using root mean square error (RMSE) (see Eq. (8)).[25,26] The RMSE and R^2 are calculated using the following equations:

$$R^2 = \frac{\sum_{k=1}^{n}\left(y_{exp} - \overline{y}_{exp}\right)\left(y_{pred} - \overline{y}_{pred}\right)}{\sqrt{\sum_{k=1}^{n}\left(y_{exp} - \overline{y}_{exp}\right)^2 \sum_{k=1}^{n}\left(y_{pred} - \overline{y}_{pred}\right)^2}} , \qquad (7)$$

$$RMSE = \sqrt{\frac{\sum_{i=1}^{n}\left(y_i^{exp} - y_i^{pred}\right)^2}{n-k}} , \qquad (8)$$

where n is the number of observations; k is the number of variables; y_{exp} and y_{pred} are the observed and the calculated values, respectively; and $\overline{y}_{exp}$ and $\overline{y}_{pred}$ are the averaged values for the observed and the calculated values, respectively.

2.5 Internal and external validation

For the validation of the predictive power of the ANN model, two basic principles (internal validation and external validation) are available. In this study, the internal validation was used to evaluate the internal predictive ability of the developed models, and its result was defined as Q^2_{LOO} (see Eq. (9))[27] and the external validation to determine both the generalizability and the true predictive ability of the ANN models for new chemicals, by splitting the available dataset into a training set and an external prediction set, and its result was defined as Q^2_{ext} (see Eq. (10)).[27]

The Q^2_{LOO} and Q^2_{ext} are calculated using the following equations:

$$Q^2_{LOO} = 1 - \frac{\sum_{i=1}^{training}\left(y_i^{exp} - y_i^{pred}\right)^2}{\sum_{i=1}^{training}\left(y_i^{exp} - \overline{y}\right)^2} , \qquad (9)$$

where y_i^{exp}, y_i^{pred}, and $\overline{y}$ are the experimental, predicted, and average of the experimental values for the training set, respectively. For $Q^2_{LOO} > 0.5$ is considered satisfactory, and for $Q^2_{LOO} > 0.9$ is excellent.[28]

$$Q^2_{ext} = 1 - \frac{\sum_{i=1}^{prediction}\left(y_i^{exp} - y_i^{pred}\right)^2}{\sum_{i=1}^{prediction}\left(y_i^{exp} - \overline{y}_{tr}\right)^2} , \qquad (10)$$

where y_i^{exp} and y_i^{pred} are the experimental and predicted values for the prediction set, respectively, and $\overline{y}_{tr}$ is the mean experimental of the experimental values for the training set.

3 Results and discussion

A range of one to six neurons in the hidden layer was obtained in the ANN models to predict the properties of dif-

Table 3 – List of pure, binary, and ternary systems used in the development of the model

N	Pure system A	Exp. data points	Refs.
1	Soybean oil, sunflower oil, rapeseed oil, grapeseed oil		21
2	Corn oil		19,21
3	BD*(n-peanut-sunflower)		12
4	Soybean FAME		11,20,23
5	BD*(rapeseed oil)		17
6	BE*	308	17,10
7	BD* (sunflower waste-frying oil), Jojoba oil		24
8	Castor oil		22
9	Soybean FAEE		23
10	Jatropha FAME, Jatropha FAEE		16

N	Binary system A–B		Refs.
11	BE*-PD		10
12	PD-BD*(n-peanut-sunflower)		12
13	PD-Soybean FAME		11
14	Soybean oil-PD, Soybean FAME-PD		20
15	PD-Soybean oil	489	18
16	BD*-Jojoba oil, PD-BD*, PD-Jojoba oil		24
17	PD-Soybean FAME, Methanol-Soybean FAME, PD-Soybean FAEE, Ethanol-Soybean FAEE		23
18	Jatropha FAME-Jatropha FAEE		16

N	Ternary system A–B–C		Refs.
19	PD-Methanol-Soybean FAME, PD-Ethanol-Soybean FAEE		23
20	PD-BD* (rapeseed oil)-Ethanol		17
21	Soybean FAME-Soybean oil-PD	342	20
22	Jatropha FAME-Jatropha FAEE-PD		16

* BD: biodiesel; BE: bioethanol; PD: petrodiesel; FAME: fatty acid methyl ester; FAEE: fatty acid ethyl ester

ferent systems. The topology of the neural network was determined by the following: the number of layers and neurons in each layer, and the nature of the transfer functions. The next section presents the most effective models that were found in this work. The STATISTICA program was used for the application of the artificial neural network. The best neural network configuration had one hidden layer with twenty-six (26) neurons (Table 4). Fig. 3 illustrates the correlation between the simulation results of the developed neural network and the experimental data points for the density and kinematic viscosity. The perfect fit (output equal to targets) is indicated by the solid line. The close proximity of the best linear fit to the perfect fit, as observed in Fig. 3, shows a good correlation among the network predictions and the experimental data ($R^2 = 0.9965$ for the density and $R^2 = 0.9938$ for the kinematic viscosity).

3.1 Mathematical expressions optimised neural models

From the optimised ANN, represented in Fig. 4, the density and kinematic viscosity of different systems can be expressed by a mathematical model that incorporates all inputs E_i (T, X_1, X_2, X_3, ρ (at 20 °C), μ (at 20 °C)) within it, as follows:

Table 4 – Selected parameters of the optimal multi-layer perceptron

| Parameters studied	RMSE (minimum value)		R^2 (maximum value)		Selected parameters
	density	kinematic viscosity	density	kinematic viscosity	
The database distribution					
(80 %) training, (10 %) test, (10 %) validation	0.0090	2.47	0.9530	0.9640	(70 %) training,
(70 %) training, (15 %) test, (15 %) validation	**0.0029**	**0.89**	**0.9955**	**0.9930**	(15 %) test, and
(60 %) training, (20 %) test, (20 %) validation	0.0087	1.99	0.9630	0.9650	(15 %) validation
Activation functions (hidden layer–output layer)					
Logistic–Logistic	0.0050	1.49	0.9830	0.9860	
Logistic–Identity	0.0052	1.39	0.9810	0.9880	
Logistic–Tanh	0.0051	1.59	0.9820	0.9850	
Tanh–Logistic	0.0052	1.42	0.9810	0.9870	
Tanh–Identity	**0.0020**	**0.86**	**0.9965**	**0.9938**	Tanh–Identity
Tanh–Tanh	0.0054	1.66	0.9800	0.9830	
Identity–Logistic	0.0078	4.45	0.9580	0.8830	
Identity–Identity	0.0071	8.93	0.9650	0.5050	
Identity–Tanh	0.0097	8.97	0.9360	0.5050	
Number of neurons in the hidden layer 1–40	0.0020	0.86	0.9965	0.9938	26 Neurons
Learning algorithms					
Quasi–Newton back propagation (BFGS)	**0.0020**	**0.86**	**0.9965**	**0.9938**	Quasi–Newton back propagation (BFGS)
Scaled conjugate gradient (SCG)	0.0070	4.12	0.9660	0.8970	
Conjugate gradient descent (CGD)	0.0087	4.44	0.9520	0.8870	
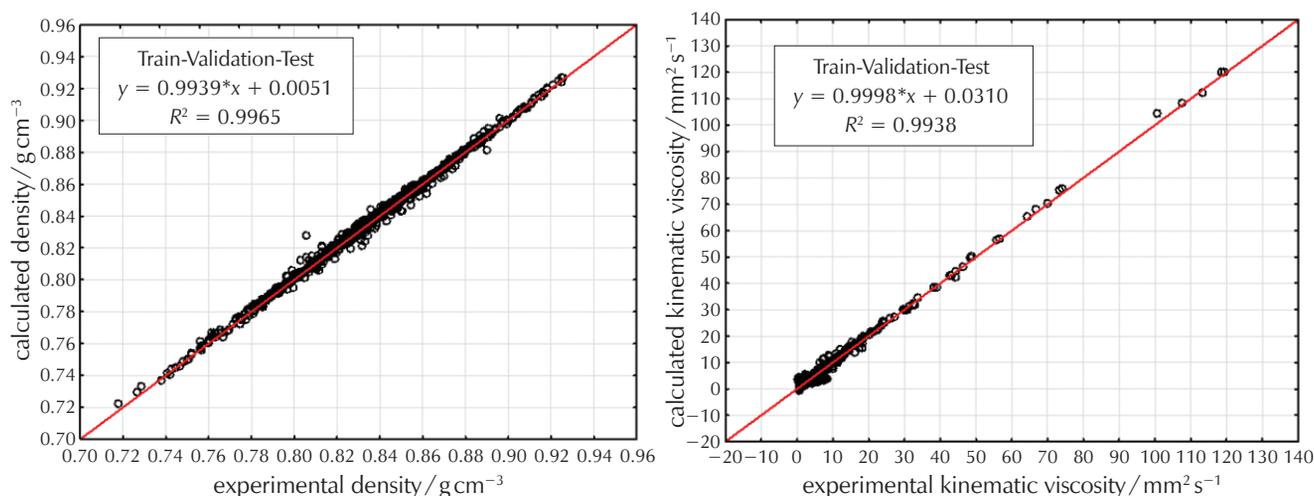
Fig. 3 – Comparison between experimental and calculated values of (a) the density, and (b) the kinematic viscosity of global system

The instance outputs z_j of the hidden layer:

$$z_j = f\left(\sum_{i=1}^{6} E_i w_{j,i} + b_j\right) = \frac{2}{1 + \exp(-2\sum_{i=1}^{6} E_i w_{j,i} + b_j)} - 1; \quad (11)$$

$$j = 1, 2, \ldots, 26.$$

The output ρ, μ:

$$\rho = \left(\sum_{j=1}^{26} v_{k1,j} z_j + b_{k1}\right), \quad (12)$$

$$\mu = \left(\sum_{j=1}^{26} v_{k2,j} z_j + b_{k2}\right). \quad (13)$$

The combination of Eqs. 11 and 12 leads to the mathematical formula for density taking into account all the inputs E_i ($T, X_1, X_2, X_3, \rho(20\ ^\circ C), \mu(20\ ^\circ C)$):

$$\rho = \left(\sum_{j=1}^{26} v_{k1,j}\left(\frac{2}{1 + \exp(-2\sum_{i=1}^{6} E_i w_{j,i} + b_j)} - 1\right) + b_{k1}\right) \quad (14)$$

The combination of Eqs. 11 and 13 leads to the mathematical formula for kinematic viscosity taking into account all the inputs E_i ($T, X_1, X_2, X_3, \rho(20\ ^\circ C), \mu(20\ ^\circ C)$):

$$\mu = \left(\sum_{j=1}^{26} v_{k2,j}\left(\frac{2}{1 + \exp(-2\sum_{i=1}^{6} E_i w_{j,i} + b_j)} - 1\right) + b_{k2}\right), \quad (15)$$

where $w_{i,j}$ represents the synaptic weight of the connection from neuron i of the input layer to neuron j in the hidden layer; $v_{k,j}$ represents the weight of synaptic connection the neuron j of the hidden layer to neuron k of the output layer; b_j and b_k represent the means of neuron j in the hidden and the neuron k of the output layer.

3.2 Statistical analysis on the ANN models for systems

The experimental and simulated values were compared using a linear regression model with a good agreement. Table 5 indicates the statistical analysis for the comparison between experimental and simulated values for the density and kinematic viscosity of different systems.

Table 5 – Statistical analysis for the comparison between experimental and simulated values

	α	β	R^2	RMSE	Q^2_{LOO}	Q^2_{ext}
$\rho/g\,cm^{-3}$	0.9939	0.0051	0.9965	0.0020	0.9960	0.9966
$\mu/mm^2\,s^{-1}$	0.9998	0.031	0.9938	0.86	0.9924	0.9960

Linear equation: $y = \alpha * x + \beta$, with α = splote, β = y-intercept

3.3 Interpolation and extrapolation performances

To check the accuracy of the two ANN models previously developed and optimised, one type of interpolation and extrapolation databases were used. The interpolation database contains a set of intermediate points between the experimental points of kinematic viscosity and density of soybean oil.[21] The extrapolation database contains a set of points outside the experimental points of kinematic viscosity and density of soybean oil.[21] The quality of fit of the interpolation data set and the extrapolation data set are depicted in Fig. 5 for the density and the kinematic viscosity. An excellent fit to the experimental values density and kinematic viscosity of soybean oil can be noted:

$$y_{exp}(at\ 140\ ^\circ C) < y_{pred}(at\ 130\ ^\circ C) < y_{exp}(at\ 120\ ^\circ C) < \ldots$$
$$< y_{pred}(at\ 15\ ^\circ C) < y_{exp}(at\ 10\ ^\circ C).$$

So, a good interpolation database for the density and the kinematic viscosity.

$$y_{pred}(at\ 150\ ^\circ C) < y_{exp}(at\ 140\ ^\circ C)\ and$$
$$y_{exp}(at\ 10\ ^\circ C) < y_{pred}(at\ 5\ ^\circ C).$$

So, a good extrapolation database for the density and the kinematic viscosity, where y_{exp} and y_{pred} are the experimental and predicted values for the density and the kinematic viscosity.

3.4 Prediction performances

Prediction performance is a method to check the accuracy of the two ANN models previously developed and optimised. A 238 database experimental of 4 systems (2 pure systems, 1 binary system, and 1 ternary system) was used for the prediction. This database was obtained from the scientific publication.[16] The results of prediction performances in terms of root mean squared error (RMSE) for density and kinematic viscosity of new systems are summa-
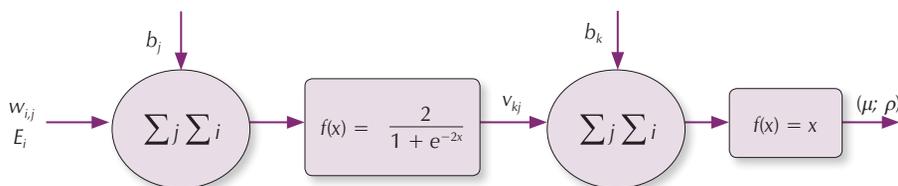

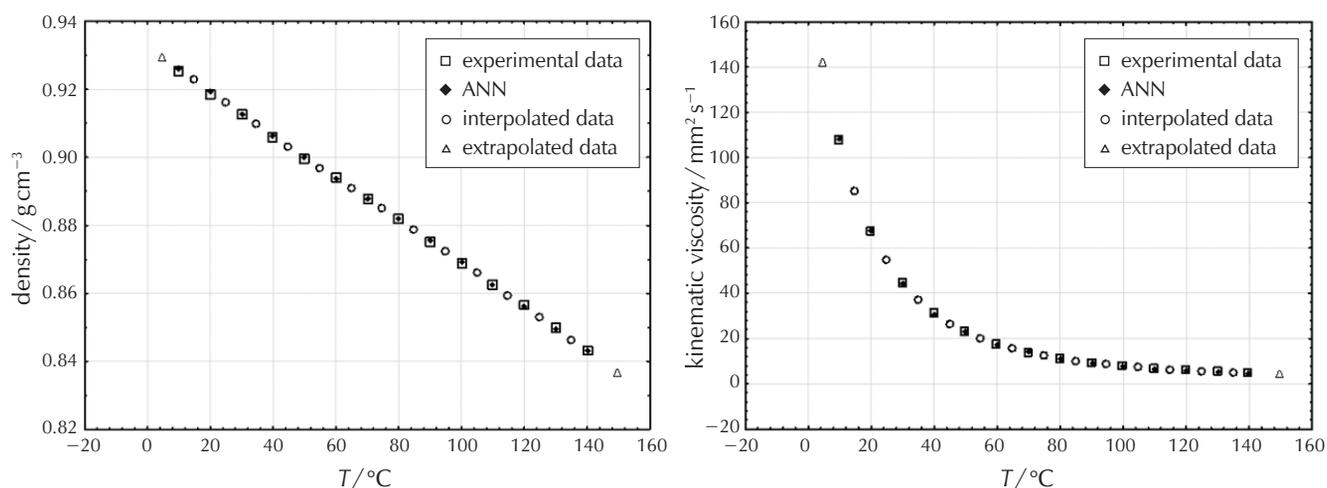Fig. 4 – Schematic representation of the optimised NN

Fig. 5 – Simulation results of the interpolation and extrapolation database for (a) the density, and (b) the kinematic viscosity of soybean oil

Table 6 – Prediction results in terms of root mean squared error (RMSE)

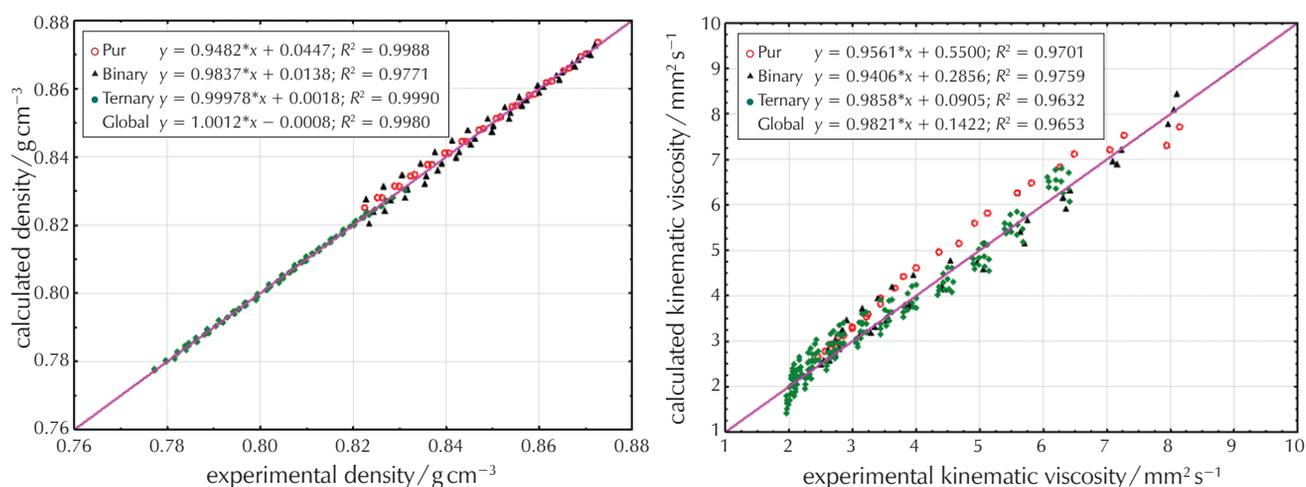| Ref.	Systems		Data point kinematic viscosity / mm² s⁻¹	RMSE	
				density / g cm⁻³	
16	pure	palm FAEE, palm FAME	28	0.08	0.0002
	binary	PalmFAME-PalmFAEE	40	0.06	0.0005
	ternary	palm FAME-palm FAEE-PD	168	0.11	0.0002
	total		238	0.14	0.0005

Fig. 6 – Simulation results of the prediction database for (a) the density, and (b) the kinematic viscosity of new systems

rised in Table 6. The quality of fit of the prediction data set is depicted in Fig. 6 for the density and kinematic viscosity. An excellent fit between the experimental values and the results obtained from the ANN model of density and kinematic viscosity of new systems ($R^2 = 0.9980$ for the density and $R^2 = 0.9653$ for the kinematic viscosity).

3.5 Comparison with unstructured kinetic models

To have a comparison between the neural networks models developed in this work with others' correlations, the diffusivity of two pure systems, a binary system, and a ternary system was estimated. Therefore, the network developed, as well as eight correlations of the different systems

Table 7 – Correlations of the comparison

Ref.	Systems	Equations	
		Density	Viscosity
16	Jatropha FAME	$\rho = 1.095 - 0.000744T$ (Eq. 28)	$\eta = 27.535 - 0.0732T$ (Eq. 32)
	Jatropha FAEE	$\rho = 1.093 - 0.000747T$ (Eq. 39)	$\eta = 27.724 - 0.0733T$ (Eq. 33)
	Jatropha FAME + Jatropha FAEE	$\rho = 1.0915 - 0.0007T + 0.0027X_1$ (Eq. 30)	$\eta = 27.7706 - 0.0734T - 0.1786X_1$ (Eq . 34)
	Jatropha FAME + Jatropha FAEE + Petro-diesel	$\rho = 1.027 - 0.0007T + 0.0666X_1 + 0.0390X_2$ (Eq. 31)	$\eta = 20.2430 - 0.0540T + 1.283X_1 + 0.910X_2$ (Eq. 35)
21		–	$\mu = \dfrac{\eta}{\rho}$ (Eq. 36)

T = temperature (K), η = dynamic viscosity (mPa.s), ρ = density (g cm^{-3}), μ = kinematic viscosity (mm^2 s^{-1}), FAME = fatty acid methyl ester, FAEE = fatty acid ethyl ester

Table 8 – Comparison of the proposed ANN model with the experimental data and other correlations of pure, binary, and ternary system for test data set

Ref.	systems				RMSE		
		kinematic viscosity / mm^2 s^{-1}			density / g cm^{-3}		
		ANN		16	ANN	16	
16	pure	Jatropha FAEE, Jatropha FAME	**0.32**	0.48	0.0015	**0.0002**	
	binary	Jatropha FAME + Jatropha FAEE	**0.20**	0.47	**0.0015**	0.0135	
	ternary	Jatropha FAME+Jatropha FAEE + Petro-diesel	**0.21**	0.35	**0.0004**	0.0014	
	global		**0.22**	0.39	**0.0007**	0.0034	

proposed by *Baroutian et al.*[16] for the density and the kinematic viscosity, were used (Table 7).

Table 8 indicates the results of this comparison and the RMS error of pure, binary, ternary, and global system for the density and the kinematic viscosity of each method separately.

Fig. 7 shows the RMS error of the proposed ANN model and processes proposed by *Baroutianet et al.*[16] used for the prediction of the density and the kinematic viscosity for all points of the test data for the three systems. As can be seen from the figure, the proposed neural network model is better than the other method for the density and kinematic viscosity, despite the proposed ANN model formed by a large database of 1025 experimental points with several pure, binary, and ternary systems, plus it proposed ANN model to estimate the density and the kinematic viscosity at the same time. The RMS error of the ANN method for all test data of the density is 0.0007 g cm^{-3}, however, in the method of *Baroutian et al.*[16] it is 0.0034 g cm^{-3}.

The RMS error of the ANN method for all test data of the kinematic viscosity is 0.22 mm^2 s^{-1}, however in the method of *Baroutian et al.*[16] it is 0.39 mm^2 s^{-1}.
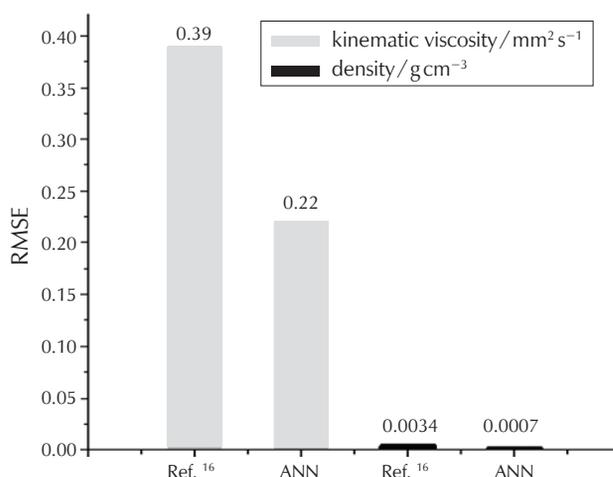

Fig. 7 – Root mean square error (RMSE) of the developed ANN model and other method used for prediction of density and kinematic viscosity in comparison to the experimental test data

4 Conclusions

New models of one artificial neural network were developed to predict the density (ρ) and kinematic viscosity (μ) of different systems of biofuels and their blends with diesel fuel from the volume fractions (X_1, X_2, and X_3) of the components, temperature (T). For difference between these systems, we used ρ (at 20 °C) and μ (at 20 °C). A set of 1025 points of experimental data for the density and the kinematic viscosity of 34 systems was used for network training. The back propagation of the neural network was done by transfer functions like tangent hyperbolic and identity for hidden layer and output layer, respectively. The BFGS algorithm was used for optimisation of the neural network. A range of one to twenty-six neurons in the hidden layer of models were obtained. In the validation stage, the results of comparison between experimental and simulated values in terms of the root mean squared error, the internal validation and the external validation for the density and the kinematic viscosity were, respectively: RMSE = 0.0020 g cm^{-3}, Q^2_{LOO} = 0.9960, Q^2_{ext} = 0.9966, and RMSE = 0.86 mm^2 s^{-1}, Q^2_{LOO} = 0.9924, Q^2_{ext} = 0.9960.

The results of applying the neural network model formed for the density and the kinematic viscosity of systems indicate that the method has very good interpolation and extrapolation capabilities with the respect to the temperature. The results of applying the neural network model formed to predict the density and kinematic viscosity of new systems (prediction) indicate that the method has good prediction for 238 new databases experimental of four systems. The results of prediction performances in terms of the root mean squared error were: RMSE = 0.0005 g cm^{-3} for density and RMSE = 0.14 mm^2 s^{-1} for kinematic viscosity. Furthermore, the comparison of validation results with those correlations proposed by *Baroutian et al.* indicated that the ANN predicted the density and kinematic viscosity more accurately than those correlations proposed by *Baroutian et al.*

List of abbreviations and symbols

ANN　– artificial neural network

T　– temperature, °C

RMSE – root mean squared error

R　– correlation coefficient

FAEE – fatty acid ethyl ester

FAME – fatty acid methyl ester

PD　– petro-diesel

BE　– bioethanol

BD　– biodiesel

BFGS – Brogden-Fletcher-Goldfarb-Shanno

SCG　– Scaled-Conjugate-Gradient

CGD　– Conjugate gradient descent

GHG　– greenhouse gas

CO_2　– carbon dioxide

ASTM – American Society for testing and materials

EN　– European norm

SLNN – single layer neural network

DNN　– deep neural network

CNN　– convolution neural network

exp　– experimental

pred　– predicted

tanh　– tangent hyperbolic

References

Literatura

1. *N. Winchester, R. Malina, M. D. Staples, S. R. H. Barrett*, The impact of advanced biofuels on aviation emissions and operations in the U.S. Energy Economics **49** (2015) 482–491, doi: https://doi.org/10.1016/j.eneco.2015.03.024.

2. *P. A. Cremonez, M. Feroldi, C. de J. de Oliveira, J. G. Teleken, H. J Alves, S. C. Sampaio*, Environmental, economic and social impact of aviation biofuel production in Brazil, New Biotechnol. **32** (2) (2015) 263–271, doi: https://doi.org/10.1016/j.nbt.2015.01.001.

3. *T. Kandaramath Hari, Z Yaakob, N. N. Binitha*, Aviation biofuel from renewable resources: Routes, opportunities and challenges, Renew. Sust. Energ. Rev. **42** (2015) 1234–1244, doi: https://doi.org/10.1016/j.rser.2014.10.095.

4. *D. A. Saldana, L. Starck, P. Mougin, B. Rousseau, N. Ferrando, B. Creton*, Prediction of density and viscosity of biofuel compounds using machine learning methods, Energ. Fuel. **26** (4) (2012) 2416–2426, doi: https://doi.org/10.1021/ef3001339.

5. *L. F. Ramírez Verduzco*, Density and viscosity of biodiesel as a function of temperature: Empirical models, Renew. Sust. Energ. Rev. **19** (2013) 652–665, doi: https://doi.org/10.1016/j.rser.2012.11.022.

6. *F. Hou, Z. Wu, Z. Hu, Z. Xiao, L. Wang, X. Zhang, G. Li*, A Comparison Study on the Prediction of Multiple Molecular Properties by Various Neural Networks, J. Phys. Chem. A **122** (46) (2018) 9128–9134, doi: https://doi.org/10.1021/acs.jpca.8b09376.

7. *S. Baroutian, M. K. Aroua, A. A. A. Raman, N. M. N. Sulaiman*, Viscosities and Densities of Binary and Ternary Blends of Palm Oil+Palm Biodiesel+Diesel Fuel at Different Temperatures, J. Chem. Eng. **55** (2010) 504–507, doi: https://doi.org/10.1021/je900299x.

8. *J C. Chavarria-Hernandez, D. E. Pacheco-Catalán*, Predicting the kinematic viscosity of FAMEs and biodiesel: Empirical models, Fuel **124** (2014) 212–220, doi: https://doi.org/10.1016/j.fuel.2014.01.105.

9. *C. I. Rocabruno-Valdés, L. F. Ramírez-Verduzco, J. A. Hernández*, Artificial neural network models to predict density, dynamic viscosity, and cetane number of biodiesel, Fuel **147** (2015) 9–17, doi: https://doi.org/10.1016/j.fuel.2015.01.024.

10. *V. Kumbár, A. Polcar*, Flow behavior of petrol, bio-ethanol and their blends, Acta Univ. Agric. Silvic. Mendelianae Brun. **60** (2012) 211–216, doi: https://doi.org/10.11118/actaun201260060211.

11. *S. H. Yoon, S. H. Park, C. S. Lee*, Experimental Investigation on the Fuel Properties of Biodiesel and Its Blends at Various Temperatures, Energ. Fuel. **22** (2008) 652–656, doi: https://doi.org/10.1021/ef7002156.

12. *L. F. Ramírez-Verduzco, B. E. García-Flores, J. E. Rodríguez-Rodríguez, A. R. Jaramillo-Jacoba*, Prediction of the density and viscosity in biodiesel blends at various temperatures, Fuel **90** (2011) 1751–1761, doi: https://doi.org/10.1016/j.fuel.2010.12.032.

13. *S. Haykin*, Neural networks: a comprehensive foundation, 2nd Ed. Prentice Hall, New Jersey, 1998.

14. *A. Rezrazi, S. Hanini, M. Laidi*, An optimisation methodology of artificial neural network models for predicting solar radiation: a case study, Theoret. Appl. Climatol. **123** (3-4) (2015) 769–783, doi: https://doi.org/10.1007/s00704-015-1398-x.

15. *C. Si-Moussa, S. Hanini, R. Derriche, M. Bouhedda, A. Bouzidi*, Prediction of high-pressure vapor liquid equilibrium of six binary systems, carbon dioxide with six esters, using an artificial neural network model, Braz. J. Chem. Eng. **25** (1) (2008) 183–199, doi: https://doi.org/10.1590/S0104-66322008000100019.

16. *S. Baroutian, K. Shahbaz, F. S. Mjalli, M. A. Hashim, I. M. Al-Nashef*, Densities and Viscosities of Binary Blends of Methyl Esters + Ethyl Esters and Ternary Blends of Methyl Esters + Ethyl Esters + Diesel Fuel from $T = $ (293.15 to 358.15) K, J. Chem. Eng. Data **57** (5) (2012) 1387–1395, doi: https://doi.org/10.1021/je2013445.

17. *I. Barabás, A. Todorut, D. Băldean*, Performance and emission characteristics of a CI engine fuelled with diesel–biodiesel–bioethanol blends, Fuel **89** (2010) 3827–3832, doi: https://doi.org/10.1016/j.fuel.2010.07.011.

18. *Z. Franco, Q. D. Nguyen*, Flow properties of vegetable oil–diesel fuel blends, Fuel **90** (2011) 838–843, doi: https://doi.org/10.1016/j.fuel.2010.09.044.

19. *I. Nita, S. Geacai*, Study of density and viscosity variation with temperature for fuels used for Diesel engine, Ovidius University Annals of Chemistry **22** (1) (2011) 57–61, url: http://citeseerx.ist.psu.edu/viewdoc/download?doi=10.1.1.227.6830&rep=rep1&type=pdf.

20. *A. A. Oluwafunmilayo, E. A. Samuel, O. A. Ayobami*, A Laboratory Study of the Effect of Temperature on Densities and Viscosities of Binary and Ternary Blends of Soybean Oil, Soy Biodiesel and Petroleum Diesel Oil, Adv. Chem. Eng. Sci. **2** (2012) 444–452, doi: https://doi.org/10.4236/aces.2012.24054.

21. *B. Esteban, J.-R. Riba, G. Baquero, A. Rius, R. Puig*, Temperature dependence of density and viscosity of vegetable oils, Biomass Bioenerg. **42** (2012) 164–171, doi: https://doi.org/10.1016/j.biombioe.2012.03.007.

22. *K. U. Mara, R. F. S. Juliana, A. Marina, B. Manuela, C. Keli, P. A. Isabella, A. M. Marcio, A. P. V. Fernando, F. C. Vladimir, C. F. Lúcio, L. C. Marcos, O. J. Vladimir*, Effect of temperature and composition on density, viscosity and thermal conductivity of fatty acid methyl esters from soybean, castor and *Jatropha curcas* oils, J. Chem. Thermodyn. **58** (2013) 460–466, doi: https://doi.org/10.1016/j.jct.2012.10.007.

23. *M. B. Silveira, F. R. do Carmo, R. S. Santiago-Aguiar, H. B. de Sant'Ana*, Ab–diesel: Liquid–liquid equilibrium and volumetric transport properties, Fuel **119** (2014) 292–300, doi: https://doi.org/10.1016/j.fuel.2013.11.022.

24. *Z. Al-Hamamre, A. Al-Salaymeh*, Physical properties of (jojoba oil + biodiesel), (jojoba oil + diesel) and (biodiesel + diesel) blends, Fuel **123** (2014) 175–188, doi: https://doi.org/10.1016/j.fuel.2014.01.047.

25. *D. A. Belsey, E. Kuh, R. E. Welsch*, Regression Diagnostics: Identifying Influential Data and Sources of Collinearity. New York: John Wiley & Sons, 1980, doi: https://doi.org/10.1002/0471725153.

26. *S. H. Hong, M. W. Lee, D. S. Lee, J. M. Park*, Monitoring of sequencing batch reactor for nitrogen and phosphorus removal using neural networks, Biochem. Eng. J. **35** (2007) 365, doi: https://doi.org/10.1016/j.bej.2007.01.033.

27. *R. Wang, J. Jiang, Y. Pan, H. Cao, Y. Cui*, Prediction of impact sensitivity of nitro energetic compounds by neural network based on electrotopological-state indices, J. Hazard. Mater. **166** (2009) 155–186, doi: https://doi.org/10.1016/j.jhazmat.2008.11.005.

28. *L. Eriksson, J. Jaworska, A. P. Worth, M. T. Cronin, R. M. McDowell, P. Gramatica*, Methods for reliability and uncertainty assessment and for applicability evaluations of classification and regression-based QSARs, Environ. Health Perspect. **111** (2003) 1361–1375, doi: https://doi.org/10.1289/ehp.5758.

SAŽETAK

Modeli umjetne neuronske mreže za predviđanje gustoće i kinematičke viskoznosti različitih sustava biogoriva i njihovih mješavina s dizelskim gorivom. Usporedna analiza

Souad Belmadani,[a*] *Salah Hanini,*[b] *Maamar Laidi,*[b] *Cherif Si-Moussa,*[b] and *Mabrouk Hamadache*[b]

U ovom članku dva modela zasnovana na metodologiji umjetne neuronske mreže (ANN) optimizirana su za predviđanje gustoće (ρ) i kinematičke viskoznosti (μ) različitih sustava biogoriva i njihovih mješavina s dizelskim gorivom. Za razvoj tih modela upotrijebljena je eksperimentalna baza podataka od 1025 točaka, uključujući 34 sustava (15 čistih sustava, 14 binarnih sustava i 5 ternarnih sustava). Ti modeli koriste šest ulaza: temperatura (T) u rasponu od −10 do 200 °C, volumni udjeli (X_1, X_2, X_3) u rasponu 0 – 1, a za razlikovanje tih sustava korištena je kinematička viskoznost pri 20 °C u rasponu 0,67 – 74,19 mm² s⁻¹ i gustoća pri 20 °C u rasponu 0,7560 – 0,9188 g cm⁻³. Najbolji rezultati dobiveni su arhitekturom {6-26-2: 6 neurona u ulaznom sloju – 26 neurona u skrivenom sloju – 2 neurona u izlaznom sloju}. Rezultati usporedbe eksperimentalnih i simuliranih vrijednosti u smislu korelacijskih koeficijenata bili su: $R^2 = 0,9965$ za gustoću i $R^2 = 0,9938$ za kinematičku viskoznost. Za provjeru točnosti dva prethodno razvijena modela ANN upotrijebljeno je 238 novih eksperimentalnih baza podataka s 4 sustava (2 čista sustava, 1 binarni sustav i 1 ternarni sustav). Rezultati performansi predviđanja s obzirom na korelacijske koeficijente bili su: $R^2 = 0,9980$ za gustoću i $R^2 = 0,9653$ za kinematičku viskoznost. Usporedba rezultata validacije s rezultatima drugih studija pokazuje da su modeli neuronske mreže dali znatno bolje rezultate.

Ključne riječi
Modeliranje, neuronska mreža, kinematička viskoznost, gustoća, biogoriva